4
Why electron scattering?

In this section we present a brief overview of the virtues of electron scattering. We revisit most of this material in detail in the remainder of the book.

There are many reasons why inclusive electron scattering (e, e') provides a powerful tool for studying the structure of nuclei and nucleons. First, the interaction is known — it is given by *quantum electrodynamics* (QED), the most accurate physical theory we have. Second, the interaction is relatively weak — of order $\alpha = 1/137.0$, the fine-structure constant, and thus one can make measurements without greatly disturbing the structure of the target. Furthermore, the interaction is with the local electromagnetic current density in the target $\hat{J}_\mu(x)$. Hence one *knows* what is measured.

The process is governed by the S-matrix, which with one photon exchange (Fig. 4.1) takes the form[1]

$$S_{fi}^{(\gamma)} = \frac{-ee_p}{\hbar c\,\Omega}\bar{u}(k_2)\gamma_\mu u(k_1)\frac{1}{k^2}\int e^{ik\cdot x}\langle f|\hat{J}_\mu(x)|i\rangle\, d^4x \tag{4.1}$$

What is measured is the Fourier transform with respect to the four-momentum transfer $\hbar k$ with $k \equiv k_1 - k_2$ of the transition matrix element of the current density.

In electron scattering, one can vary the three-momentum transfer and energy transfer *independently* in

$$\begin{aligned} k &= (\boldsymbol{\kappa}, i\omega/c) \\ \boldsymbol{\kappa}^2 &= (\mathbf{k}_1 - \mathbf{k}_2)^2 \\ \hbar\omega &= \varepsilon_1 - \varepsilon_2 \end{aligned} \tag{4.2}$$

For a given energy transfer, one can map out the three-dimensional Fourier transform with respect to $\boldsymbol{\kappa}$ of the transition densities. The inversion of

[1] We quantize with periodic boundary conditions in a big box of volume Ω and in the end let $\Omega \to \infty$.

https://doi.org/10.1017/9781009290616.006 Published online by Cambridge University Press

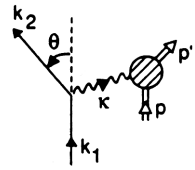

Fig. 4.1. Kinematics for electron scattering (e, e′) with one photon exchange.

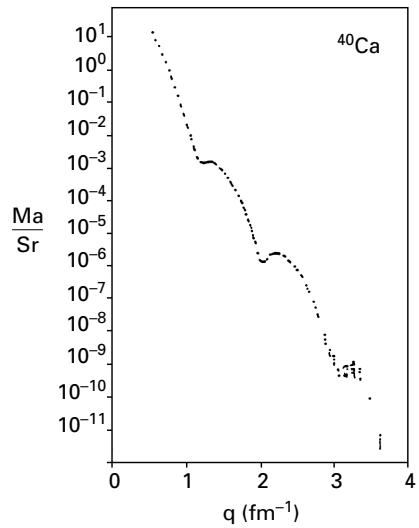

Fig. 4.2. Cross section for elastic electron scattering ^{40}Ca(e, e) vs. momentum transfer (here $q \equiv \kappa$) [Fr79].

this Fourier transform than provides the *microscopic spatial distribution of the densities.*

We give an example in Fig. 4.2. This is the diffraction pattern observed when electrons are scattered elastically from ^{40}Ca. The data are from Saclay [Fr79]. Notice the central diffraction maximum and the series of concentric rings with decreasing intensity as the scattering angle is increased. Notice also the scale on the ordinate; it runs over 13 decades. Figure 4.3 [Ho81, Se86] shows the charge distribution obtained upon inversion of the Fourier transform. The abscissa is in fermis.[2] The band in the experimental data is an estimate of the uncertainty introduced by the fact that one, by necessity, only measures a partial Fourier transform. The

[2] The situation is actually somewhat more complicated than this. As Z gets large, the distortion of the incident and outgoing electron wave functions by the Coulomb field of the nucleus must be taken into account, and one must perform a partial wave analysis of Coulomb scattering from the nuclear charge distribution.

https://doi.org/10.1017/9781009290616.006 Published online by Cambridge University Press

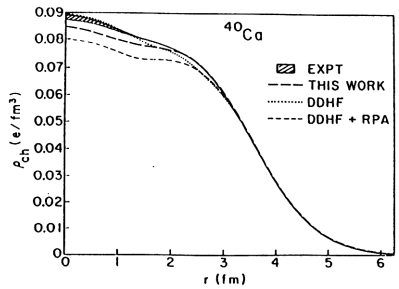

Fig. 4.3. Charge distribution of ^{40}Ca obtained from Fig. 4.2 with estimate of measurement error. Units are 1 fm $= 10^{-13}$ cm. Heavy dashed curve shows calculation in relativistic mean field theory (RMFT) in QHD (other curves show similar results in traditional approach) [Ho81, Se86].

theoretical curves give an indication of the present level of understanding of these charge densities in nuclear physics.

Recall that there is an *inverse relationship* between the three-momentum transfer and the distance scale at which one probes the system

$$|\boldsymbol{\kappa}| = \frac{2\pi}{\lambda} \tag{4.3}$$

In electromagnetic studies in nuclear physics one focuses on how matter is put together from its constituents and on distance scales ~ 10 fm to ~ 0.1 fm. Particle physics concentrates on finer and finer details of the substructure of matter with experiments at high energy which in turn explore much shorter distances.

In electron scattering, one can moreover vary the polarization of the virtual photon in Fig. 4.1 by changing the electron kinematics; through this, the charge and current interaction can be separated. In sum, electron scattering gives rise to a precisely defined virtual quantum of electromagnetic radiation, and hence electrons provide a *precision tool* for examining the structure of nuclei and nucleons. Of course, an additional great advantage of electrons is that they can be copiously produced in the laboratory, and since they are charged, they can readily be accelerated and detected.[3]

Electron scattering is furthermore a versatile tool. One knows from the theory of electromagnetism that two currents will interact with each other. The moving electron produces such a current. Thus not only is there a Coulomb interaction between the charged electron and the charges in the target, but there is also a magnetic interaction between the moving electron and the current in the target. The nuclear current is produced

[3] Neutrino scattering for example, which has similar virtues for the weak interaction, lacks these properties.

https://doi.org/10.1017/9781009290616.006 Published online by Cambridge University Press

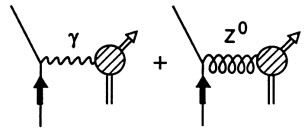

Fig. 4.4. (e, e′) amplitude as sum of γ and Z^0 exchange.

both by the convection current of the moving protons and also by the curl of the intrinsic magnetization, arising from the fact that nucleons are themselves little magnets; electron scattering measures the full transition matrix element of the target current

$$J_\lambda(x) \quad = \quad [\mathbf{J}_c(x) + \nabla \times \boldsymbol{\mu}(x),\ i\rho(x)] \tag{4.4}$$

In addition, with electron scattering one has the possibility of bringing out high multipoles of the current at large values of κR.

The interference between γ and Z^0 exchange (Fig. 4.4), where Z^0 is the heavy boson mediating the weak neutral current interaction, gives rise to *parity violation*. One measure of parity violation is the asymmetry arising from the difference in cross section of right- and left-handed electrons in inclusive electron scattering ($\vec{\mathrm{e}}, \mathrm{e}'$)

$$\mathscr{A} \quad \equiv \quad \frac{d\sigma_\uparrow - d\sigma_\downarrow}{d\sigma_\uparrow + d\sigma_\downarrow} \tag{4.5}$$

The S-matrix for the amplitude in Fig. 4.4 takes the form[4]

$$S_{fi} \quad = \quad S_{fi}^{(\gamma)} - \left(\frac{\hbar}{c}\right)^2 \frac{G}{\sqrt{2}\,\Omega} \bar{u}\gamma_\mu(a + b\gamma_5)u \int e^{ik\cdot x} \langle f|\hat{\mathscr{J}}_\mu^{(0)}(x)|i\rangle\, d^4x \tag{4.6}$$

where

$$\langle f|\hat{\mathscr{J}}_\mu^{(0)}(x)|i\rangle \quad = \quad \langle f|\hat{J}_\mu^{(0)}(x) + \hat{J}_{\mu 5}^{(0)}(x)|i\rangle \tag{4.7}$$

Here $\hat{\mathscr{J}}_\mu^{(0)}(x)$ is the weak neutral current operator for the target and $G = 1.027 \times 10^{-5}/m_p^2$ is Fermi's weak coupling constant. Parity violation arises from the interference of the first term in Eq. (4.6) with the two contributions linear in the axial vector current in the second. If the first term has been measured and is assumed known, then the parity-violation asymmetry measures the second. Hence parity violation in ($\vec{\mathrm{e}}, \mathrm{e}'$) *doubles* the information content in electron scattering as it provides a means of

[4] In the standard model of the electroweak interactions $a = -(1 - 4\sin^2\theta_W)$ and $b = -1$ [Wa95].

https://doi.org/10.1017/9781009290616.006 Published online by Cambridge University Press

measuring the spatial distribution of weak neutral current in nuclei and nucleons.

The cross section for inclusive electron scattering (e, e') with one photon exchange is characterized by two response surfaces (see below) which are each functions of two Lorentz invariants. These invariants can be taken to be the four-momentum transfer squared $\hbar^2 k^2$ and the scalar product $\nu \equiv -k \cdot p / M_T$ where $\hbar p$ is the initial four-momentum of the target, m_T its mass, and M_T is its inverse Compton wavelength.

$$M_T \equiv \frac{m_T c}{\hbar} \qquad M \equiv \frac{m_p c}{\hbar} \tag{4.8}$$

The second invariant ν, when evaluated in the laboratory frame where the target is initially at rest, reduces to the energy loss of the electron $\nu = \hbar\omega_{\text{lab}}/\hbar c$. The deep-inelastic region (DIS) for electron scattering from the nucleon is defined by letting $k^2 \to \infty$ and $\nu \to \infty$ while keeping their *ratio* $x \equiv k^2/2M\nu$ fixed. In deep-inelastic scattering the two response surfaces are observed to satisfy *Bjorken scaling*. They become independent of k^2 and are finite functions of the single variable x [Bj69, Fr72]. There is no form factor for the constituents from which one is scattering in this region. DIS provided the first dynamical evidence for the point-like quark substructure of hadrons. It also provides a measurement of the quark momentum distribution. Furthermore, QCD predictions for the $\ln k^2$ corrections in the approach to scaling can also be tested in DIS [Ro90].

The initial experiments at SLAC on parity violation in DIS [Pr78, Pr79] gave the first clear evidence that the weak neutral current has the structure predicted by the standard model of the electroweak interactions.

Further experiments, originated at SLAC, on the scattering of polarized electrons by polarized nucleons [Hu83] allow one to examine the strong-interaction spin structure functions of the nucleon.